MFN= 007101
01 SID/SCD
02 5689
03 INPE-5689-PRE/1846
04 CEA
05 S
06 as
10 Clemesha, Barclay Robert
10 Sahai, Yogeshwar
10 Simonich, Dale Martin
10 Takahashi, Hisao
12 Comment on "Nighttime Na D emision observed from a polar-orbiting DMSP satellite" by A.L. Newman
14 6601-6606
30 Journal of Geophysical Research
31 95
32 A5
40 En
41 En
42 <E>
58 DAE
58 DGE
61 <PI>
64 May <1990>
68 PRE
76 AERONOMIA
83 In a recent paper, Newman [1988] has presented Na D airglow profiles obtained by a limb-scanning instrument aboard one of the DMSP satellites. These profiles show a number of surprising features. The unexpected characteristics of the satellites measurements are (1) surprisingly high intensities at the equator, as compared with midnorthern latitudes; (2) topside scale heights for the emission intensity as large as 16 km; and (3) peak emission heights as low as 75 km..
90 b
91 FDB-19960311
92 FDB-MLR

JOURNAL OF GEOPHYSICAL RESEARCH, VOL. 95, NO. A5, PAGES 6601-6606, MAY 1, 1990

COMMENT ON "NIGHTTIME NA D EMISSION OBSERVED FROM A POLAR-ORBITING DMSP SATELLITE" BY A. L. NEWMAN

B. R. Clemesha, Y. Sahai, D. M. Simonich, and H. Takahashi

Instituto de Pesquisas Espaciais, São José dos Campos
São Paulo, Brazil

In a recent paper, Newman [1988] has presented Na D airglow profiles obtained by a limb-scanning instrument aboard one of the DMSP satellites. These profiles show a number of surprising features. The unexpected characteristics of the satellite measurements are (1) surprisingly high intensities at the equator, as compared with mid-northern latitudes; (2) topside scale heights for the emission intensity as large as 16 km; and (3) peak emission heights as low as 75 km.

Observations

The Emission Intensities

The measured intensities were about a factor of 3 greater at the equator than at 40°N. On the basis of ground-based measurements of the sodium nightglow this result is unexpected. Although it is true that winter intensities are generally higher than summer, the main variation is semiannual, with maxima close to the equinoxes. It should be noted that the seasonal variations in Na D airglow are quite different from those in sodium density, which shows a strong winter maximum [Simonich et al., 1979]. The maximum July D2 line intensities measured by Kirchhoff and Takahashi [1985] at Natal (6°S) were less than 20 R, with average values of about 10 R. Data for higher latitudes are available from many stations, including São José dos Campos (23°S), Haleakala (21°N), Kitt Peak (32°N), Abastumani (41°N), and Haute Provence (44°N). Early measurements from Sacramento Peak, Haute Provence, and Tamanrasset, which used wideband filters, were subject to contamination and may not be reliable. There is a great dispersion in the measured values, but the lowest summer values for São José dos Campos are about 25 R [Kirchhoff et al., 1981a], and for Kitt Peak and Haleakala the July values are around 10 to 15 R [Ciner and Smith, 1973]. Work by Smith and Steiger [1968] and Wiens and Weill [1973] suggests that there is little difference between mid- and low-latitude Na D airglow intensities in July. Fukuyama [1977] compares measurements from Haute Provence, Abastumani (41°N), Haleakala, and Davao (7°N). July values, scaled from Fukuyama's Figure 8, are 40, 40, 25 and 35 R for 44°, 41°, 20°, and 7°, respectively, for the sum of the D1 and D2 lines. A comparison of recent, carefully calibrated, simultaneous measurements at Fortaleza (4°S) and Cachoeira Paulista (23°S) suggests that average Na D intensities are typically a factor of 3 greater at the latter station than near the equator [Takahashi et al., 1989]. It is difficult to compare measurements made at different locations and different times, but all the published data suggest that, at the most, the intensities should be similar at mid-northern latitudes and the equator in July, and more probably the equatorial airglow would be weaker.

Paper number 89JA02861.
0148-0227/90/89JA-02861$02.00

Topside Scale Heights

The topside scale heights for the emission, measured by the satellite, vary from just over 6 km near the equator to nearly 16 km at 50°N. Typical values at mid-latitudes are 10 - 12 km. Assuming that the Chapman mechanism is responsible for the excitation of the sodium atoms, then the scale height for the emission intensity will depend on the vertical gradients in both sodium and ozone. Over the past 20 years, lidar measurements have provided a great deal of accurate data for the vertical distribution of free sodium atoms. There can be no doubt that the typical topside scale height of the free sodium is of the order of 3 km, considerably less than that of the main atmospheric constituents in the relevant height range. Our knowledge of the ozone distribution is much less precise, but both measurements [Green et al., 1986] and models [Shimazaki and Laird, 1970] suggest that the ozone density decreases with a scale height roughly similar to that of the main atmospheric components, except in the region of 85 km, where it shows a secondary maximum. This suggests that in the region of 100 km the topside scale height for the emission should normally be less than 3 km, since both sodium and ozone would be decreasing in the relevant height range. To get a scale height for the emission as large as 10 km would require the ozone to increase with height above the sodium peak with an e-folding distance not much greater than the scale height for the sodium. This is a very improbable situation.

Peak Emission Heights

The tangent heights for peak emission, as measured by the satellite, vary from about 90 km at 40°N to 77 km at the equator, with minimum values around 75 km at 10°N. Lidar profiles of free sodium almost always show negligible concentration below 80 km [Simonich et al., 1979; Gardner et al., 1986; Nomura et al., 1987], so it should not be possible for the emission to peak below this height. There is considerable evidence that the emission normally peaks in the region of 88 km. This conclusion is based on rocket measurements [Heppner and Meredith, 1958], model calculations [Kirchhoff et al., 1981b], and measurements of the propagation of gravity waves through the emitting layer [Clemesha et al., 1978; Takahashi et al., 1979, 1985].

Analysis

In view of the unexpected nature of most of the parameter variations derived from the satellite measurements, it is important to make an attempt to determine to what extent these variations reflect real characteristics of the sodium airglow. There are three factors which have not been considered in the analysis presented by Newman [1988]. Firstly, the analysis does not take into account the possible contamination signals which might be seen by the photometer. Secondly, the data are presented as a function of tangent height, with no attempt to make allowance for the varying path length seen by the photometer in the spherical shell formed by the emitting layer. Thirdly, no allowance has been made for optical extinction of the airglow emission along its path within the sodium layer.

Contamination

According to Newman [1988] the satellite photometer used a filter centered on 5890 Å, with a bandwidth of 57 Å. The Na D lines are not the only atmospheric emissions to be expected in this spectral region. Within the bandwidth of the filter are the OH(8,2) Q, R, and P branches, and the NO_2 continuum emissions. The R branch, centered on 5870 Å, represents about 25% of the entire band emission, Q1(1) at 5888 Å about 15%, Q1(2) at 5895 Å about 4%, and P1(2) at 5915 Å about 7%. According to Llewellyn et al. [1978] the total band intensity should be of the order of 15 R, so we should expect about 7 R within the photometer passband. Our own measurements, in which we measure the R branch intensity in order to estimate the Q branch contamination of our measured Na D intensities, show intensities typically twice this value. We should expect, then, a total contamination of the order of 10 R from the OH(8,2) band. Rocket-borne photometer measurements of the NO_2 continuum have been made by McDade et al. [1986], who found zenith intensities of the order of 0.5 R $Å^{-1}$ at 5400 Å and 7140 Å. For the 57-Å filter we should thus expect a contribution of about 30 R. Taking the OH and NO_2 intensities together we should then expect a total contamination of about 40 R. This must be compared with zenith airglow intensities which, for equatorial and northern summer conditions, would be expected to be of the order of 10 to 30 R. Thus we can see that the contamination from OH and NO_2 probably contributes not less than 50% to 75% of the glow measured by the satellite photometer. This may well be an underestimate, because the sodium airglow seen by the satellite suffers the effects of extinction by the sodium layer, whereas the OH and NO_2 emissions do not.

Geometrical Corrections and Extinction

The analysis of limb-scanning measurements of atmospheric layers has been undertaken by a number of workers (see, for example, Yee and Abreu [1987]), and adequate techniques exist for inverting the experimental data to retrieve the vertical layer profile. The case of the sodium emission is complicated by the fact that the sodium layer is not optically thin at the Na D line wavelengths. Resonant extinction of the emission leads to a continuous change in its spectrum as the light propagates through the sodium layer, and this must be taken into account when calculating the intensity loss. The total extinction thus depends on the initial spectrum of the sodium emission, as well as the wavelength dependent extinction coefficient and the total column abundance of sodium between the emitting region and the satellite. Since most of the sodium atoms in the layer will be in the ground state, the wavelength dependence of the extinction coefficient can be assumed to be that corresponding to sodium atoms at a temperature of about 200 K. The emission spectrum, on the other hand, appears to correspond to a much higher temperature. Sipler and Biondi [1978] have measured the spectrum of sodium nightglow and have shown that it corresponds to a temperature of about 700 K. They ascribe this to excess energy released in the chemical excitation process which puts the sodium atoms into the ^2P state.

In order to illustrate the effects of the geometrical factors and the extinction, we have computed the limb intensities as a function of tangent height for a number of hypothetical cases. In all computations we have assumed that the airglow emission corresponds to sodium atoms at 700 K, and that the extinction is by atoms at 200 K. Simonich and Clemesha [1983] have analyzed the effects of resonant extinction on lidar returns, and we have followed a similar analysis in our computations. The computations were carried out for a Gaussian layer in which the emission intensity and the sodium density were assumed to vary with height in the same way. In practice one should expect the emission profile to be centered on a height lower than that of the sodium density distribution, but lacking a detailed knowledge of the appropriate ozone distributions there is not a great deal of point in trying to achieve a closer approximation to reality. In any case, serious errors would only be introduced for very large sodium abundances. The emission layer is assumed to have the form

$$I(z) = kNa(z) = A\exp(-(z-z_0)^2/H^2)$$

where I(z) and Na(z) are the volume emission rate and sodium density, respectively, at height z; k and A are constants; and H, the "scale height," is the distance from the layer peak at which the intensity or density falls to 1/e of its maximum value. The computation includes the effects of a 5-km-wide instrument function.

In Figure 1 we show the results for a layer having a 6-km scale height centered on 88 km. The limb brightness, computed for the sum of the D1 and D2 lines, is expressed as the ratio of the limb intensity to the intensity which would be measured by a zenith-pointing photometer below the layer. Curves a through c show the computed limb brightness ratios for three different vertical sodium column abundances, and curve d shows the effect of neglecting extinction. Curve e shows, on an arbitrary scale, the assumed vertical emission profile. There are a number of points of interest in Figure 1. Firstly it can be seen that, on the topside of the layer, the limb brightness varies with tangent height in a manner quite similar to the model emission pro-

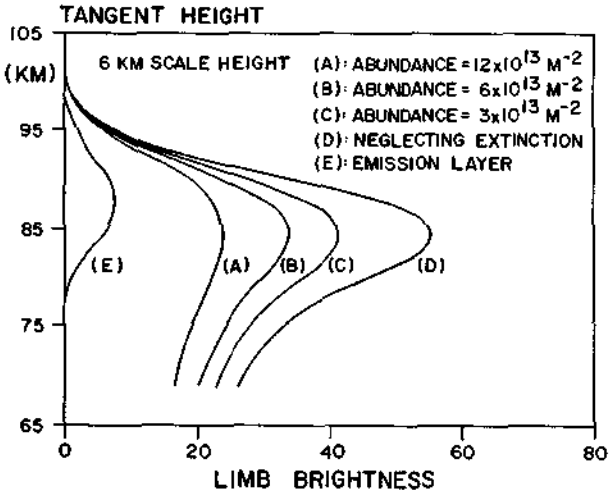

Fig. 1. Limb brightness (expressed as the ratio of limb brightness to zenith intensity) as a function of tangent height for a Gaussian layer with 6-km 1/e half width, centered on 88 km, for four different column abundances of sodium. Curve e shows the sodium density profile.

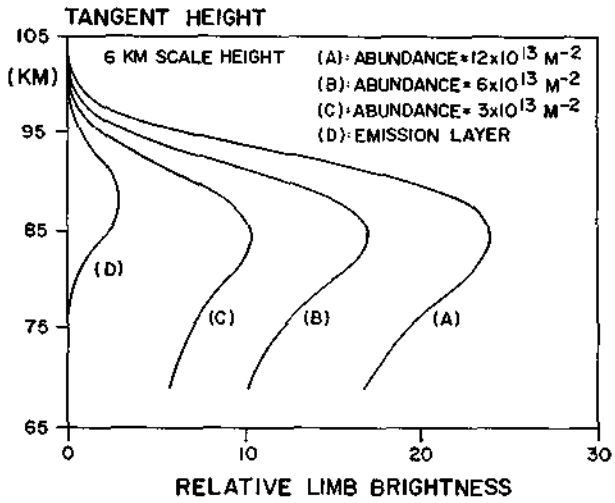

Fig. 2. Relative limb brightnesses as a function of tangent height for sodium layers having three different Na column abundances: curve a $3x10^{13}$ m^{-2}; curve b $6x10^{13}$ m^{-2} curve c $12x10^{13}$ m^{-2}.

file. In other words, taking the topside limb brightness as being representative of the actual emission profile does not lead to gross errors of interpretation. Secondly, the height of peak limb brightness is about 3.5 km below the emission peak for low abundances, but becomes closer to the true peak height as the abundance increases: this is the result of the greater extinction suffered by the emission from the lower part of the layer. Thirdly, for moderate to high abundances, extinction has a major effect on the peak limb brightness. Typical abundances of the order of 3 to $6x10^{13}$ m^{-2} lead to reductions in limb brightnesses of the order of 30%. Abundances between 6 and $12x10^{13}$ m^{-2}, however, more than halve the observed intensity. This is more clearly illustrated in Figure 2, where we show how the limb brightness profiles change with the total column abundance of sodium. In this figure the limb brightness is not normalized to the zenith intensity, but is expressed in the same, arbitrary units for each of the three abundances. Doubling the Na abundance from 6 to $12x10^{13}$ m^{-2} results in about the same increase in limb brightness as changing it from 3 to $6x10^{13}$ m^{-2}; i.e., over the range of abundances used, the peak intensity increases roughly logarithmically with peak sodium density.

Discussion

The question which must now be addressed is that of whether the effects described above can explain any of the unexpected features of the satellite measurements.

Low Peak Emission Heights

The simulations shown in Figures 1 and 2 show that the limb scan geometry results in a lowering of the apparent peak emission height of not more than about 4 km. The assumption of a broader layer would lead to a larger depression of the apparent peak height, but the low equatorial emission heights are observed together with rather narrow layers, so there appears to be no justification for such an assumption. The equatorial scans show peak tangent heights as low as 75 km, so even when the appropriate allowance is made for the viewing geometry, the true peak emission height would not be greater than 80 km. At first sight it might seem that this discrepancy could result from the effects of contamination. The main source of contamination should be the NO_2 continuum, but, according to McDade et al's [1986] results, this should peak at around 100 km and be negligible below about 85 km. OH contamination is only a slightly better candidate. Rocket measurements (see, for example, McDade et al. [1987]) typically put the peak emission between 85 and 90 km, and, as in the case of sodium, the emission should be negligible below 80 km.

Newman [1988] attempts to reproduce a profile with a low peak emission height in her Figure 14. By a suitable combination of ozone and sodium profiles she gets the peak emission to come from about 82 km. She achieves this, however, by using an unrealistic ozone profile, having a narrow secondary peak at 82 km with a full width of only about 3 km. Neither modeling studies nor measurements have ever shown such a narrow distribution. The secondary peak which is believed to occur in the ozone distribution is considerably wider than that assumed by Newman. The sodium profile used by Newman is also unrealistic in that it involves far more sodium below 80 km than has been measured by lidar.

We must conclude, then, that neither contamination nor the viewing geometry can explain the observed peak tangent heights below 80 km.

Large Scale Heights

As we have already pointed out, it is very difficult for the topside scale height of the emission profile to be larger than that of the sodium concentration, typically of the order of

3 km. As can be seen from Figure 1, the viewing geometry does not have a marked effect on the apparent topside scale height. The minimum scale height observed should be similar to the instrument function half width: 3 km in the case of the DMSP instrument. This is illustrated in Figure 3, where we have simulated the limb scan of a 1-km-thick block layer, centered on 88 km, by a photometer having a 5-km full-width rectangular instrument function. As can be seen from the figure, in this extreme case the topside scale height is about 3 km, and the tangent height of the peak limb intensity occurs about 2 km below the true peak height. Once the emission scale height is greater than the half width of the instrument function, the latter has little effect on the apparent scale height. This implies that the true minimum scale heights of the emission observed by the satellite instrument were never much less than 6 km and frequently

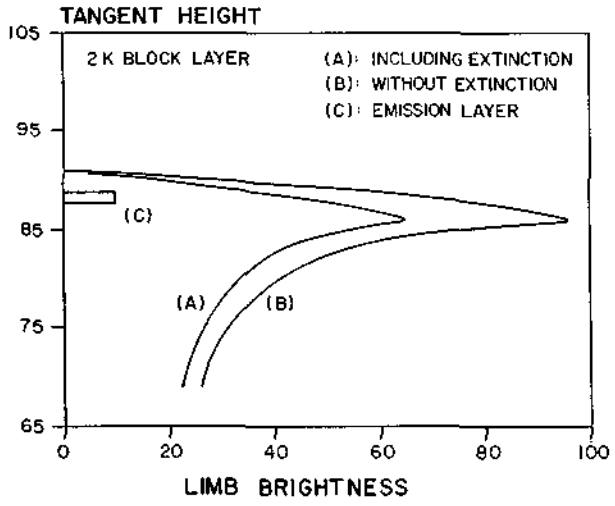

Fig. 3. Limb brightness (expressed as the ratio of limb brightness to zenith intensity) as a function of tangent height for a 1-km-thick block layer.

were much more. Contamination, on the other hand, could well have a major effect on the measured scale heights. As we have already pointed out, the main contaminating emission should be the NO_2 continuum, which according to McDade et al.'s [1986] measurements, peaks at about 100 km and has a topside scale height approaching 10 km. As we have already seen, within the passband of the satellite photometer the NO_2 continuum is likely to contribute a signal equal to or greater than the Na D emission. This means that above a tangent height of 90 km the signal measured by the photometer would have been mostly due to the NO_2 emission. As a result of this the topside scale heights determined by fitting a Chapman function to the experimental data would be controlled by the NO_2 continuum, and not the Na. It seems highly probable, then, that the large topside scale heights seen by the satellite photometer really refer to contaminating emissions, mainly NO_2, and are not related to the Na D line nightglow.

High Equatorial Intensities

It is difficult to fully explain the high intensities observed at low latitude on the basis of any of the effects discussed. It is true that we would expect higher limb intensities to be associated with the thinner emission layers seen at low latitudes. That this is the case can be seen from Figure 4, where we show simulated limb brightness profiles for Gaussian layers having half widths of 3, 6, and 12 km, respectively. As

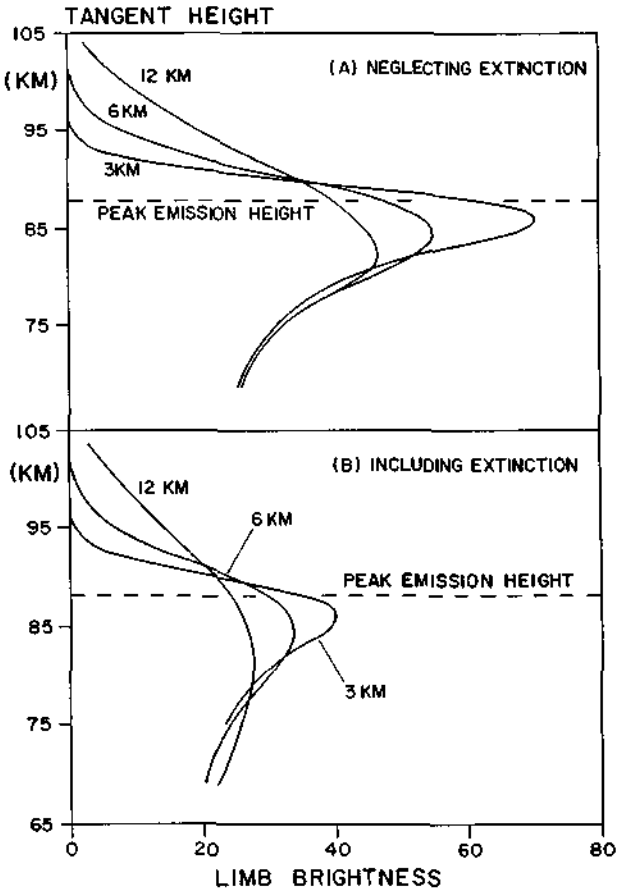

Fig. 4. Limb brightness (expressed as the ratio of limb brightness to zenith intensity) as a function of tangent height for layers with three different 1/e half widths: (a) neglecting extinction; (b) including the effects of extinction by a sodium layer with 6×10^{13} m^{-2} column abundance.

can be seen from the figure, the peak ratio of limb to zenith intensity is greatest for the thinnest layer, but this effect decreases as the column abundance increases. Furthermore, the fact that the tangent height of the low-latitude peak was lower than that of the mid-latitude emission means that it would have suffered greater extinction as a result of the longer path length through the sodium layer. This means that if the emission being measured was really sodium, and leaving aside the effects of layer thickness, then the latitudinal gradient of the emission intensity would have had to be even greater than that registered by the satellite.

Conclusions

From the simulations presented above, it can be seen that only the large topside scale heights are amenable to a simple explanation: i.e., that the signal registered by the satellite photometer was heavily contaminated by the NO_2 continuum emission. Indeed, our estimates of the relative contributions by the Na D lines and other contaminating emissions suggest that Na D may well have made only a minor contribution to the total limb brightness registered by the instrument. In this case the satellite limb-scanning measurements do not constitute a very useful contribution to our knowledge of atmospheric sodium and the Na D airglow. On the other hand, we are unable to explain on this basis the high intensity and low peak tangent height of the emission observed at low latitudes. If the sodium emission really peaks at about 80 km at low latitudes, then either the ozone density at this height must be much larger than present models and measurements suggest, or we must revise our ideas about the chemistry of atmospheric sodium and the mechanism responsible for the sodium airglow. A third possibility, that the vertical sodium distribution at low latitudes showed large values in the region of 80 km at the time that the satellite measurements were made, seems highly unlikely. Lidar measurements from as far as 78°N [Gardner et al., 1988] down to 70°S [Nomura et al., 1987] all show negligible sodium below 80 km. Similar low-altitude, high-intensity peaks were observed by the satellite over a latitude range of 30° on two nights, six days apart. The probability that they were the result of an anomalous sodium distribution seems to be negligible.

With regard to the possibility that the ozone distribution was such as to make the airglow peak close to 80 km, this, again, seems unlikely. In Figure 5 we have taken an average sodium profile for our lidar measurements (at 23°S), shown as a broken line, and multiplied by various exponential ozone profiles with scale heights as indicated in the figure. Even with an ozone scale height as low as 3 km the peak emission height is nearly 85 km. Both models and measurements on the other hand indicate nighttime ozone profiles either with scale heights greater than that of the main atmospheric constituents, i.e., greater than about 5 km, or with a minimum around 80 km. On this basis it seems almost impossible that a sodium emission profile peaking at 80 km or below, as indicated by the satellite measurements, could be produced by the Chapman mechanism with any reasonable ozone profile.

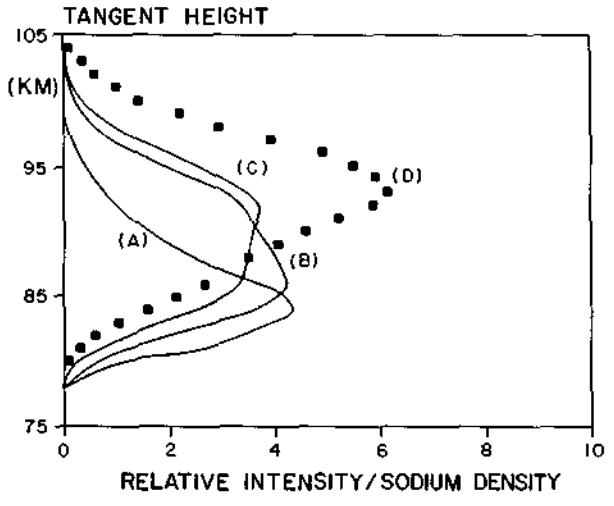

Fig. 5. Emission rates as a function of height for an average Na layer and three different ozone scale heights: curve a 3 km; curve b 6 km; curve c 9 km. The observed sodium distribution is shown as curve d. Note that the scale for intensity or sodium density is arbitrary, with different scales for the three ozone scale heights.

On the basis of the above discussion we must conclude that either the satellite measurements do not provide true profiles of the sodium airglow or the mechanism which produces the emission is quite different from that which has hitherto been assumed. Although it would appear that the measurements probably suffered very serious contamination effects, it is not possible to explain the very low peak emission heights on this basis. In view of the theoretical implications of a possible Na D emission peak at around 80km, it is important to obtain more information on the vertical distribution of the Na D emission, especially at low latitudes.

Acknowledgments. We are grateful to our colleague P. P. Batista for helpful discussions. This work was partially supported by the Fundo Nacional de Desenvolvimento Científico e Tecnológico (FNDCT) under contract FINEP-537/CT.

References

Ciner, E., and L. L. Smith, Night airglow zenith intensity variations at El Leoncito Observatory, Argentina, J. Geophys. Res., 78, 1654-1662, 1973.

Clemesha, B. R., V. W. J. H. Kirchhoff, and D. M. Simonich, Simultaneous observations of the Na 5893-Å nightglow and the distribution of sodium atoms in the mesosphere, J. Geophys. Res., 83, 2499-2503, 1978.

Fukuyama, K. Airglow variations and dynamics in the lower thermosphere and upper mesosphere, II, Seasonal and long-term variations, J. Atmos. Terr. Phys., 39, 1-14, 1977.

Gardner, C. S., D. G. Voelz, C. F. Sechrist, and A. C. Segal, Lidar studies of the nighttime sodium layer over Urbana, Illinois, 1, Seasonal and nocturnal variations, J. Geophys. Res., 91, 13659-13673, 1986.

Gardner, C. S., D. C. Senft, and K. H. Kwon, Lidar observations of substantial sodium depletion in the summertime arctic mesosphere, Nature, 332, 142-143, 1988.

Green, B. D., W. T. Rawlins, and R. M. Nadile, Diurnal variability of vibrationally excited mesospheric ozone as observed during the SPIRE mission, J. Geophys. Res., 91, 311-320, 1986.

Hays, P. B., G. R. Carignan, B. C. Kennedy, G. G. Shepherd, and J. C. G. Walker, The visible airglow experiment on Atmosphere Explorer, Radio Sci., 8, 369-377, 1973.

Heppner, J. P., and L. H. Meredith, Nightglow emission altitudes from rocket measurements, J. Geophys. Res., 63, 51-65, 1958.

Kirchhoff, V. W. J. H., B. R. Clemesha, and D. M. Simonich, Average nocturnal and seasonal variations of sodium nightglow at 23°S, 46°W, Planet. Space Sci., 29, 765-766, 1981a.

Kirchhoff, V. W. J. H., B. R. Clemesha, and D. M. Simonich, The atmospheric neutral sodium layer, 1, Recent modeling compared to measurements, J. Geophys. Res., 86, 6892-6898, 1981b.

Kirchhoff, V. W. J. H., and H. Takahashi, First sodium nightglow results for Natal, Planet. Space Sci., 33, 757-760, 1985.

Llewellyn, E. J., B. H. Long, and B. H. Solheim, The quenching of OH*, Planet. Space Sci., 26, 525-531, 1978.

McDade, L. C., E. J. Llewellyn, R. G. H. Greer, and D. P. Murtagh, ETON 3: Altitude profiles of the nightglow continuum at green and near infrared wavelengths, Planet. Space Sci., 34, 801-810, 1986.

McDade, L. C., E. J. Llewellyn, D. P. Murtagh, and R. G. H. Greer, Eton 5: Simultaneous rocket measurements of the OH Meinel v = 2 sequence and (8,3) band emission profiles in the nightglow, Planet. Space Sci., 35, 1137-1147, 1987.

Newman, A. L., Nighttime Na D emission observed from a polar-orbiting DMSP satellite, J. Geophys. Res., 93, 4067-4075, 1988.

Nomura, A., T. Kano, Y. Iwasaka, H. Fukunishi, T. Hirasawa, and S. Kawaguchi, Lidar observations of the mesospheric sodium layer at Syowma station, Antarctica, Geophys. Res. Lett., 14, 700-703, 1987.

Shimazaki, T., and A. R. Laird, A model calculation of the diurnal variation in minor neutral constituents in the mesosphere and lower thermosphere including transport effects, J. Geophys. Res., 75, 3221-3235, 1970.

Simonich, D. M., and B. R. Clemesha, Resonant extinction of lidar returns from the alkali metal layers in the upper atmosphere, Appl. Opt., 22, 1387-1389, 1983.

Simonich, D. M., B. R. Clemesha, and V. W. J. H. Kirchhoff, The mesospheric sodium layer at 23°S: Nocturnal and seasonal variations, J. Geophys. Res., 84, 1543-1550, 1979.

Sipler, D. P., and M. A. Biondi, Interferometric studies of the twilight and nightglow sodium D-line profiles, Planet. Space Sci., 26, 65-73, 1978.

Smith, L. L., and W. R. Steiger, Night airglow intensity variations in the OI 5577 Å, OI 6300 Å and NaD 5890-96 Å emission lines, J. Geophys. Res., 73, 2531-2538, 1968.

Takahashi, H., P. P. Batista, B. R. Clemesha, D. M. Simonich, and Y. Sahai, Correlations between OH, Na D and OI 5577 Å emissions in the airglow, Planet. Space Sci., 27, 801-807, 1979.

Takahashi, H., P. P. Batista, Y. Sahai, and B. R. Clemesha, Atmospheric wave propagation in the mesopause region observed by the OH(8,3) band, Na D, OA (8645 Å) band and OI 5577 Å nightglow emissions, Planet. Space Sci., 33, 381-384, 1985.

Takahashi, H., Y. Sahai, B. R. Clemesha, D. M. Simonich, N. R. Teixeira, R. M. Lobo, and A. Eras, Equatorial mesospheric and F-region airglow emissions observed at 4 degrees S, Planet. Space Sci., 37, 649-655, 1989.

Wiens, R. H., and G. Weill, Diurnal, annual and solar cycle variations of hydroxyl and sodium nightglow intensities on the Europe-Africa sector, Planet. Space Sci., 21, 1011-1027, 1973.

Yee, J. H., and V. J. Abreu, Mesospheric 5577 green line and atmospheric motions - Atmosphere Explorer satellite observations, Planet. Space Sci., 35, 1389-1395, 1987.

B. R. Clemesha, Y. Sahai, D. M. Simonich, and H. Takahashi, INPE, Av. dos Astronautas, 1758, Caixa Postal 515, 12201 São José dos Campos, São Paulo, Brazil.

(received May 31,1989;
revised August 16,1989;
accepted August 21,1989.)